Transformation of quiescent adult oligodendrocyte precursor cells into malignant glioma through a multistep reactivation process

Rui Pedro Galvao[a], Anita Kasina[a], Robert S. McNeill[b], Jordan E. Harbin[c], Oded Foreman[d], Roel G. W. Verhaak[e], Akiko Nishiyama[f], C. Ryan Miller[b,g], and Hui Zong[a,h,1]

[a]Institute of Molecular Biology, University of Oregon, Eugene, OR 97403; [b]Department of Pathology and Laboratory Medicine, University of North Carolina School of Medicine, Chapel Hill, NC 27599; [c]Department of Biological Sciences, California Polytechnic State University, San Luis Obispo, CA 93401; [d]Department of Pathology, Genentech, South San Francisco, CA 94080; [e]Department of Genomic Medicine, Department of Bioinformatics and Computational Biology, University of Texas MD Anderson Cancer Center, Houston, TX 77030; [f]Department of Physiology and Neurobiology, University of Connecticut, Storrs, CT 06269; [g]Lineberger Comprehensive Cancer Center, Neurosciences Center, and Department of Neurology, University of North Carolina School of Medicine, Chapel Hill, NC 27599; and [h]Department of Microbiology, Immunology, and Cancer Biology, University of Virginia, Charlottesville, VA 22908

Edited by Ben A. Barres, Stanford University School of Medicine, Stanford, CA, and approved August 28, 2014 (received for review August 1, 2014)

How malignant gliomas arise in a mature brain remains a mystery, hindering the development of preventive and therapeutic interventions. We previously showed that oligodendrocyte precursor cells (OPCs) can be transformed into glioma when mutations are introduced perinatally. However, adult OPCs rarely proliferate compared with their perinatal counterparts. Whether these relatively quiescent cells have the potential to transform is unknown, which is a critical question considering the late onset of human glioma. Additionally, the premalignant events taking place between initial mutation and a fully developed tumor mass are particularly poorly understood in glioma. Here we used a temporally controllable Cre transgene to delete *p53* and *NF1* specifically in adult OPCs and demonstrated that these cells consistently give rise to malignant gliomas. To investigate the transforming process of quiescent adult OPCs, we then tracked these cells throughout the premalignant phase, which revealed a dynamic multistep transformation, starting with rapid but transient hyperproliferative reactivation, followed by a long period of dormancy, and then final malignant transformation. Using pharmacological approaches, we discovered that mammalian target of rapamycin signaling is critical for both the initial OPC reactivation step and late-stage tumor cell proliferation and thus might be a potential target for both glioma prevention and treatment. In summary, our results firmly establish the transforming potential of adult OPCs and reveal an actionable multiphasic reactivation process that turns slowly dividing OPCs into malignant gliomas.

cancer | cellular quiescence | cellular reactivation | mTOR signaling

The quiescence and reactivation of progenitor cells play essential roles in tissue homeostasis, regeneration, and cancer (1–5). As tissues mature, progenitor cells often enter a quiescent state characterized by greatly reduced proliferation relative to embryonic levels, although they can be transiently reactivated into high levels of proliferation by physiologic stimuli or signals for tissue repair. Although most progenitors become increasingly quiescent with aging (6–9), cancer incidence is highest in seniors, suggesting a critical role of cellular reactivation for tumorigenesis. Because not all cell types can be equally activated (10–13), identifying the cell of origin for adult cancers and understanding the mechanisms of their reactivation should provide critical insights for cancer prevention and treatment.

Malignant gliomas are devastating, incurable brain tumors, and particularly little is known about the early stages of their development. Recently, we showed that perinatal oligodendrocyte precursor cells (OPCs) can give rise to glioma upon the loss of *p53* and *neurofibromatosis 1* (*NF1*) (14), two of the most frequently mutated tumor suppressor genes in human glioblastoma (GBM) (15, 16). However, the transforming potential of perinatal OPCs could result from a synergy between genetic lesions and the rapid proliferation of OPCs at this age. Compared with their perinatal counterparts, adult OPCs are relatively quiescent (9, 17–19). Although all adult OPCs retain the ability to proliferate, they do so at a very slow rate, dividing only once in 36 d at P60 (60-d-old mice) compared with every 4 d at P6 (9, 19). Furthermore, adult OPCs adopt a transcriptional program with much decreased expression of cell cycle genes (20, 21), thus contributing to their infrequent proliferation. Reactivation of adult quiescent OPCs has been previously characterized in response to neuronal activity and to brain injury, both of which trigger proliferation followed by differentiation into myelinating oligodendrocytes (22–24), but never in the context of oncogenic mutations. Because 87% of human malignant gliomas occur after 55 y of age (25), it is necessary to investigate whether adult OPCs can be transformed into tumors, and if so, how they become reactivated. Mechanisms regulating progenitor cell quiescence are beginning to emerge (1, 26), including the mammalian target of rapamycin (mTOR) pathway, which has known functions in normal OPC biology (27–30). If adult OPCs can form gliomas, such pathways might play important roles in the tumorigenic process.

Here we focused on adult high-grade gliomas rather than pediatric gliomas, which are molecularly and clinically distinct

Significance

How malignant gliomas arise in a mature brain remains a mystery, which hinders the development of effective treatments. Which cell types can escape their quiescent, adult state and how they do so is unknown. Additionally, because gliomas are only detected at advanced stages, the full course of transformation remains uncharacterized. Here we report that adult oligodendrocyte precursor cells, despite their relatively quiescent properties, can be reactivated to a highly proliferative state by *p53* and *NF1* mutations and give rise to malignant gliomas. Furthermore, we describe the early phase of gliomagenesis for the first time, revealing a multistep process of reactivation, dormancy, and final transformation in which mammalian target of rapamycin signaling plays a critical role at both early and late steps.

Author contributions: R.P.G., R.S.M., C.R.M., and H.Z. designed research; R.P.G., A.K., R.S.M., and J.E.H. performed research; A.N. contributed new reagents/analytic tools; R.P.G., A.K., R.S.M., J.E.H., O.F., and R.G.W.V. analyzed data; and R.P.G. and H.Z. wrote the paper.

The authors declare no conflict of interest.

This article is a PNAS Direct Submission.

Data deposition: The microarray data reported in this paper have been deposited in the Gene Expression Omnibus (GEO) database, www.ncbi.nlm.nih.gov/geo (accession nos. GSE61282 and GSE26676).

[1]To whom correspondence should be addressed. Email: hz9s@virginia.edu.

This article contains supporting information online at www.pnas.org/lookup/suppl/doi:10.1073/pnas.1414389111/-/DCSupplemental.

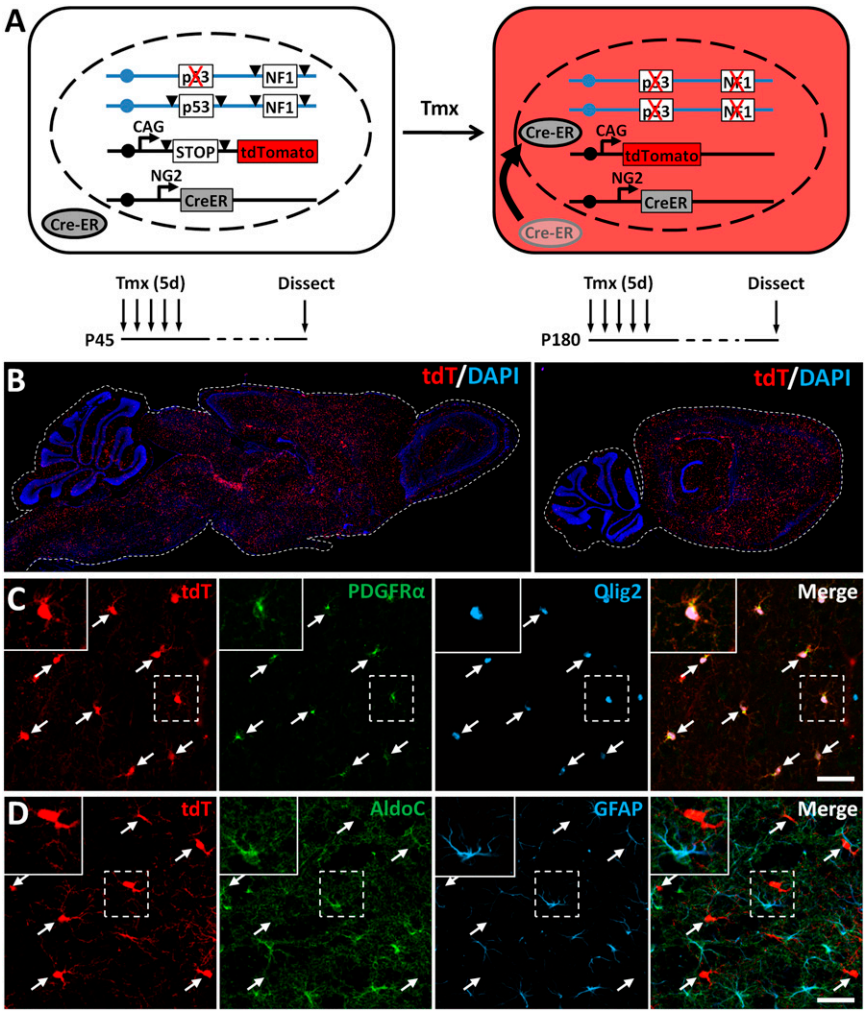

Fig. 1. Glioma mouse model using inducible NG2-CreER to specifically mutate adult OPCs. (*A*) Before tamoxifen (Tmx) administration, all cells are *p53* heterozygous ($p53^{KO/flox}$), *NF1* WT ($NF1^{flox/flox}$), and colorless because CreER is sequestered in the cytoplasm. To induce mutations in floxed *p53* and *NF1* alleles and expression of the tdTomato (tdT) reporter transgene, Tmx was given for 5 d, starting at P45 or P180, causing CreER protein in $NG2^+$ cells to enter the nucleus. Mice were then killed at different dpi depending on the experimental purpose. (*B*) Sagittal sections of mouse WT whole brain given 5 d Tmx at P45 and killed 1 d later, showing that recombination (tdT^+ cells) is evenly distributed throughout all brain regions. (*C* and *D*) Immunohistochemical characterization of tdT^+ cells showing that recombination occurs in OPCs ($PDGFR\alpha^+$, $Olig2^+$) (*C*) but not in astrocytes (Aldolase-C^+, $GFAP^+$) (*D*). (Scale bars, 40 μm.)

(31, 32). Therefore, we inactivated *p53* and *NF1* specifically in adult OPCs and found that these cells consistently give rise to malignant gliomas. Interestingly, we found that gliomagenesis from adult OPCs is not a simple linear process. Upon mutation, OPCs become immediately reactivated, reaching the proliferative rate of perinatal OPCs. Rather than continue to proliferate, mutant OPCs return to a dormancy state, until eventually one or a few cells escape dormancy for a second time, and malignant transformation ensues in specific brain regions. Knowledge of this process could yield novel opportunities to halt the progression of gliomagenesis. To exploit that possibility, we tested the role of mTOR signaling and found that it is critical for both initial OPC reactivation and later-stage tumor cell proliferation, making this pathway a good candidate for both glioma therapy and prevention.

Results

Establishing a Model to Examine the Transforming Potential of Adult OPCs. To determine whether adult OPCs can be transformed into gliomas, we established a model that contains (*i*) an NG2-CreER transgene to excise floxed alleles specifically in OPCs in a tamoxifen (Tmx)-dependent fashion (33), (*ii*) floxed alleles of *p53* and *NF1* ($p53^{KO/flox}$,$NF1^{flox/flox}$), two of the most frequently mutated tumor suppressor genes in human glioma (15), and (*iii*) a Cre-inducible reporter gene, ROSA26-LSL-tdTomato (tdT), to identify recombined cells (Fig. 1*A*). We will refer to mice with homozygous conditional *p53* and *NF1* mutations as conditional KOs (CKOs) and to their controls (no *p53* or *NF1* mutations) as WT. To induce mutations specifically in adults, we administered Tmx at either 45 or 180 d of age (young or aged adults).

To ensure that our model targets mutations to OPCs in the adult, we first confirmed the temporal and cell type specificity of the NG2-CreER transgene. To test the temporal specificity of NG2-CreER, we analyzed the brains of adult mice not given Tmx and found very few tdT^+ cells, whereas 5 d of Tmx yielded many labeled cells (Fig. S1*A*), indicating that CreER activity is highly dependent on Tmx administration. Labeled cells were distributed evenly throughout the brain, with slightly fewer in the cerebellum (Fig. 1*B*), consistent with the known distribution of OPCs in the adult brain (34). These results suggest that our approach targets OPCs without spatial bias. To test the cell type specificity of NG2-CreER, we characterized all tdT^+ cells 1 d after a 5-d Tmx treatment (5 dpi). The majority of tdT^+ cells are platelet-derived growth factor (PDGF) receptor α ($PDGFR\alpha)^+$ OPCs (72.1 ± 1.4% SEM in olfactory bulb, $n = 3$ mice; Fig. 1*C*). Other tdT^+ cells are mostly $PDGFR\beta^+$ pericytes (Fig. S1*B*), a nonneural cell type known to express NG2, as well as some $CC1^+$ oligodendrocytes (Fig. S1*C*), which likely differentiated from labeled OPCs. No tdT^+ astrocytes were detected (Fig. 1*D*). Although rare, tdT^+ cortical pyramidal neurons were also found (Fig. S1*D*); their labeling likely indicates a low level of NG2-CreER transgene expression directly in mature neurons (33) because our experimental timing is too short and too late for cortical neurogenesis to occur. We conclude that our mouse model effectively targets mutations to adult OPCs without spatial bias.

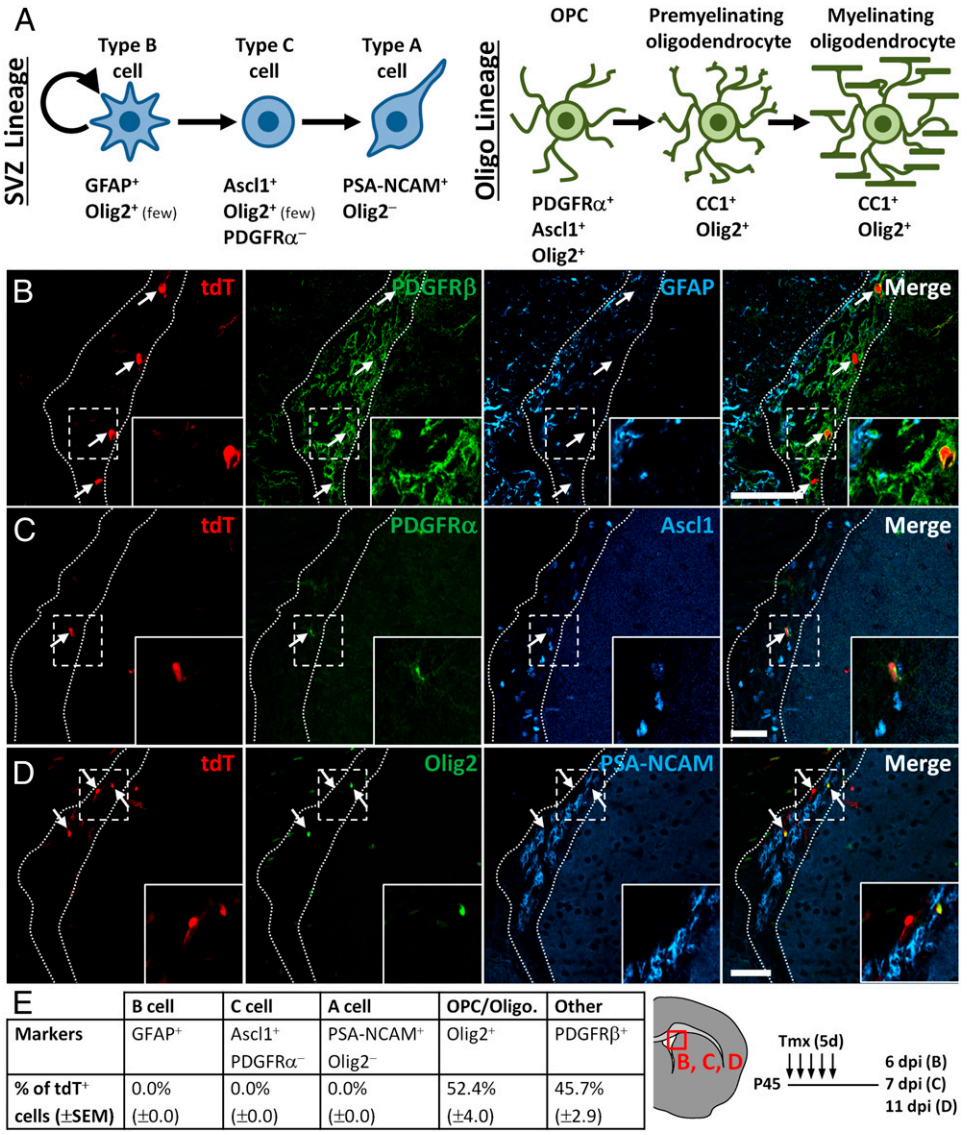

E	B cell	C cell	A cell	OPC/Oligo.	Other
Markers	GFAP+	Ascl1+ PDGFRα−	PSA-NCAM+ Olig2−	Olig2+	PDGFRβ+
% of tdT+ cells (±SEM)	0.0% (±0.0)	0.0% (±0.0)	0.0% (±0.0)	52.4% (±4.0)	45.7% (±2.9)

Fig. 2. NG2-CreER does not target adult SVZ neural stem cells. (*A*) Diagrams illustrating the cell types in the SVZ and oligodendrocyte lineages and the molecular markers used to identify them. (*B–D*) WT mice were given Tmx for 5 d at P45 and then killed 2 d (6 dpi; *B*), 3 d (7 dpi; *C*), or 7 d (11 dpi; *D*) later, allowing sufficient time for each cell type to be labeled or generated (85). Brains were then immunostained to detect tdT$^+$ cells expressing markers of type B (GFAP, *B*), type C (Ascl1, *C*), or type A cells (PSA-NCAM, *D*) in the SVZ. DAPI nuclear staining (omitted for simplicity) was used to define the boundaries of the cell-dense SVZ (dotted lines). PDGFRα, expressed by OPCs but not C cells, was used to distinguish these cell types (both can be Ascl1$^+$). Olig2, expressed by OPCs but not A cells, was used to distinguish these cell types (both can be PSA-NCAM$^+$). (*E*) Quantification results, showing that tdT$^+$ cells in the SVZ are either in the oligodendrocyte lineage or likely pericytes (PDGFRβ$^+$), but not part of the SVZ stem cell lineage (n = 4 mice for type A cells, n = 3 mice for others). (Scale bars, 50 μm.)

NG2-CreER Does Not Target Adult Neural Stem Cells. Although our data above reinforced the reliability of our mouse model, to unambiguously determine the transformation potential of adult OPCs, it is particularly important to ensure that NG2-CreER does not label adult neural stem cells (NSCs), which are known to give rise to glioma upon oncogenic mutations (35). To address this question, we first characterized tdT$^+$ cells in the subventricular zone (SVZ), the largest stem cell niche in the adult brain. The SVZ contains GFAP$^+$ (glial fibrillary acidic protein) NSCs (type B cells), which generate Ascl1$^+$ transient amplifying cells (type C cells) that differentiate into PSA-NCAM$^+$ neuroblasts (36) (type A cells; Fig. 2*A*). We found no tdT$^+$ cells within the SVZ that could be identified as type B (GFAP$^+$), type C (Ascl1$^+$/PDGFRα$^-$), or type A (PSA-NCAM$^+$/Olig2$^-$) cells (Fig. 2 *B–E*), strongly suggesting that SVZ NSCs are not labeled by NG2-CreER. In a complementary experiment, we analyzed the olfactory bulb (OB), the final destination of SVZ NSC-derived neuroblasts, for signs of adult-generated neurons derived from tdT$^+$ NSCs (Fig. S2). We administered BrdU (5-bromo-2′-deoxyuridine) to adult WT mice to label newly generated cells (Fig. S2*E*) and stained for BrdU and NeuN (Neuronal Nuclei, neuron marker) at 51 dpi (Fig. S2 *C* and *D*), when all NSC-derived neurons would have migrated to the OB and matured (37, 38). If NG2-CreER mediates recombination in NSCs, we would expect to see a population of newly formed tdT$^+$ OB neurons (tdT$^+$/BrdU$^+$/NeuN$^+$). Although we found many new neurons (BrdU$^+$/NeuN$^+$), none of them were tdT$^+$, suggesting that NG2-CreER does not induce recombination in SVZ NSCs. Based on both SVZ and OB analyses, we conclude that NG2-CreER does not induce recombination in SVZ NSCs.

Adult OPCs Generate Malignant Gliomas upon *p53/NF1* Mutation. Having confirmed the reliability of our mouse model, we next

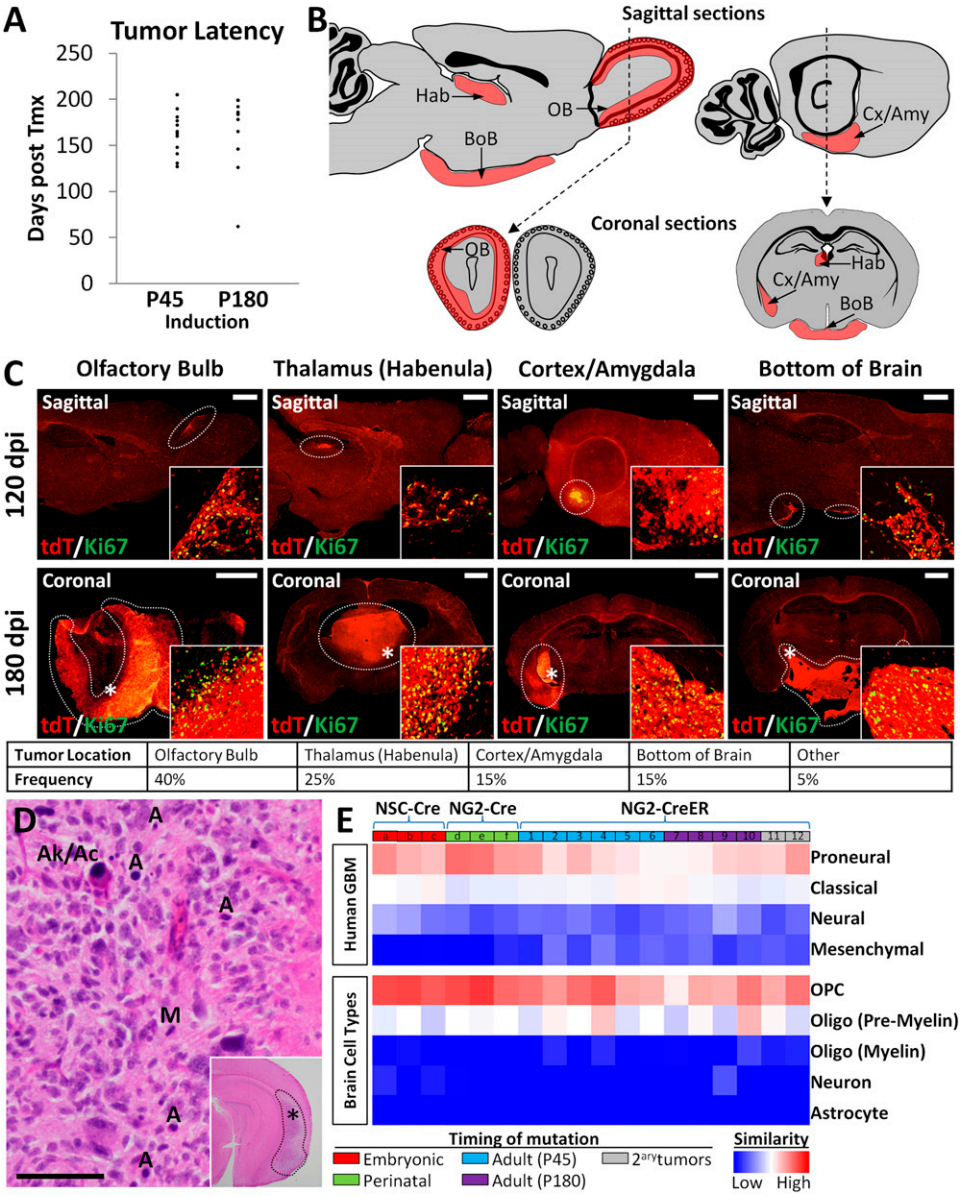

Fig. 3. Adult OPCs consistently give rise to malignant proneural gliomas in defined brain regions. (*A*) Tmx-treated mice developed brain tumors between 120 and 200 dpi in all but one case (62 dpi, P180 induction), regardless of the age of induction (P45, $n = 15$ mice, or P180, $n = 11$ mice). (*B*) Tumors were found in a few defined regions, as illustrated on diagrams of sagittal (*Upper*) and coronal (*Lower*) sections. These regions include the olfactory bulb (OB), habenula (Hab), bottom of the brain (BoB), and the area spanning the piriform cortex and amygdala (Cx/Amy). Dotted lines mark the cross sections from which the coronal diagrams are derived. (*C*) Examples of early- (120 dpi) and late-stage (180 dpi) tumors in the brain regions illustrated in the diagrams. Early-stage tumors are shown on sagittal sections and late-stage tumors on coronal sections. All tumors contained many actively dividing ($Ki67^+$) cells (*Insets*, taken from area marked by asterisk in 180 dpi examples). Quantification of tumor locations (table) was performed at 120 dpi and showed that the OB is the most common location ($n = 20$ tumors in 11 brains). (*D*) H&E staining of section containing tumor in the Cx/Amy, showing multiple features of anaplastic, malignant gliomas, such as high cellularity, invasiveness, mitotic figures (M), apoptotic cells (A), and nuclear and cellular atypias (Ak/Ac) ($n = 6$ tumors). (*Inset*) Tumor location (dotted line) in coronal hemisection; asterisk marks location of high magnification image. (*E*) Transcriptome comparison (ssGSEA) between tumor samples and the four subtypes of human glioblastoma (GBM) reveals similarity between OPC-derived gliomas and human proneural GBM subtype. Glioma samples were also compared with gene expression signatures of five neuroglial cell types (Oligo: oligodendrocyte), showing that all OPC-derived gliomas are most similar to OPCs, consistent with their cellular origin (NSC-Cre: Neural Stem Cell-Cre, includes two Nestin-Cre and one hGFAP-Cre samples; NSC-Cre and NG2-Cre ssGSEA data were previously published (14) and are provided here for comparison). [Scale bars, (*C*) 1 mm and (*D*) 20 μm.]

tested if adult OPCs can give rise to gliomas. We induced *p53/NF1* loss of function mutations at two different adult ages (P45 and P180) using the 5-d Tmx administration scheme. In both cases, CKO mice developed tdT^+ masses in the brain with 100% penetrance between 120 and 200 dpi, with the exception of one early tumor at 62 dpi (Fig. 3*A*), whereas untreated control mice never did (Table S1), confirming the adult onset of our glioma mouse model. Cells in tdT^+ masses are actively proliferating (Fig. 3*C* and Fig. S3*E*) and H&E staining showed that all masses manifest typical features of malignant anaplastic glioma, including high cellularity, mitotic figures, apoptotic cells, invasiveness, and cellular and nuclear atypia (Fig. 3*D*). Although NG2-CreER can also introduce mutations into pericytes, no histopathological features of hemangio-pericytoma were detected, making it unlikely that these tumors are derived from pericytes. It should also be noted that these tumors are likely astrocytomas and

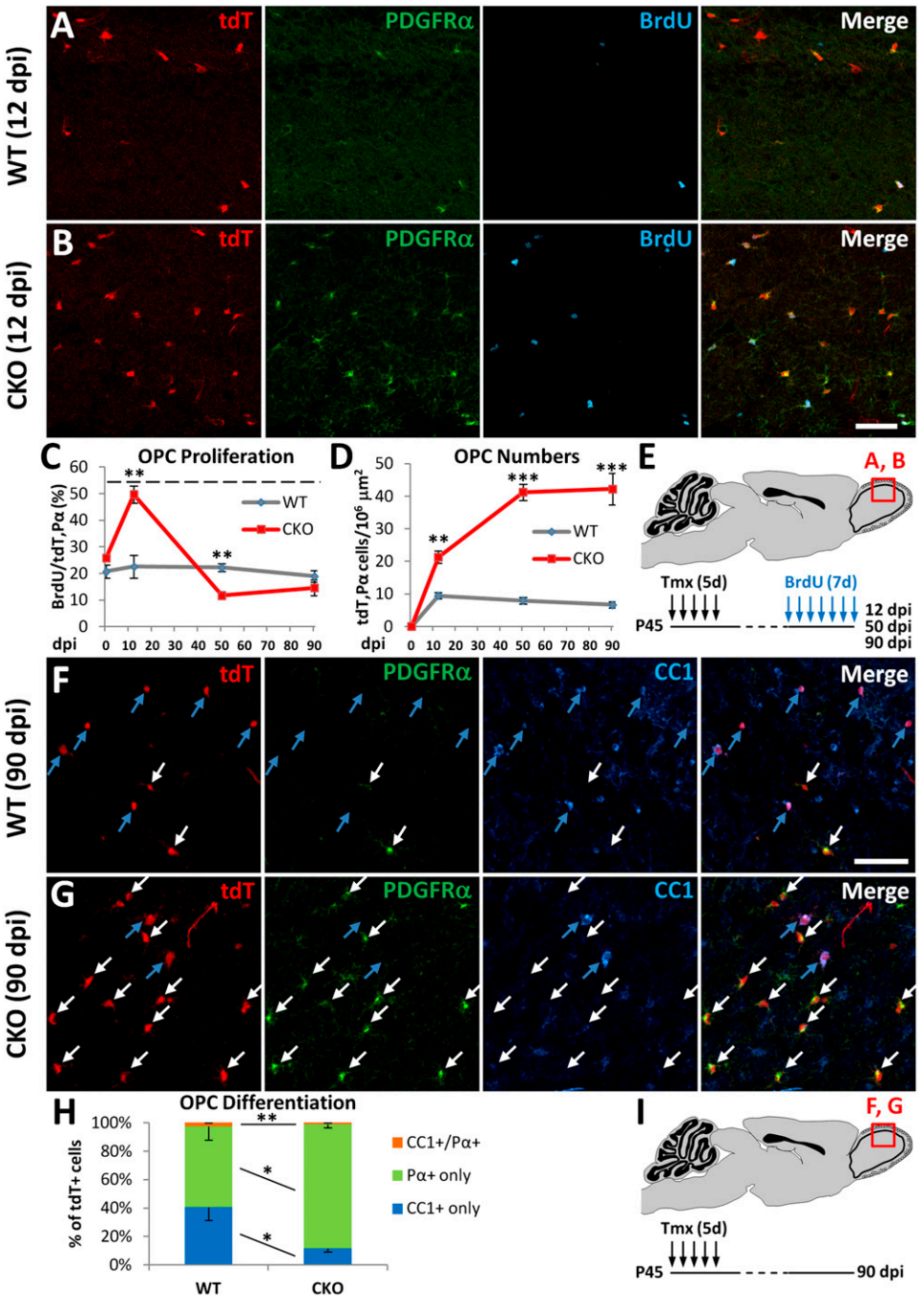

Fig. 4. Reactivation of mutant OPCs upon NG2-CreER–mediated mutagenesis. (*A* and *B*) Representative images of OB sagittal sections from 12 dpi WT (*A*) and CKO (*B*) mice immunostained for the reporter gene (tdT), an OPC marker (PDGFRα), and a proliferation marker (BrdU). (*C*) Quantification of the fraction of proliferating tdT$^+$ OPCs in the OB at various time points starting before Tmx was administered (0 dpi), as well as 12, 50, and 90 dpi, revealing a transient spike in mutant OPC proliferation at 12 dpi (for 0 dpi, proliferation was quantified among all PDGFRα$^+$ cells; no tdT$^+$ cells). Dashed line, proliferation level of perinatal (P6) OPCs (n = 4). (*D*) Quantification in the OB of the total number of tdT$^+$ OPCs starting before Tmx was administered (0 dpi), as well as 12, 50, and 90 dpi, showing that mutant OPCs accumulate throughout the premalignant phase, even after the proliferative rate returns to basal level (n = 4). (*E*) Location of images shown in *A* and *B* and diagram of experimental procedure. (*F* and *G*) Representative images of OB sagittal sections from 90 dpi WT (*F*) and CKO (*G*) mice immunostained for an OPC marker (PDGFRα) and a mature oligodendrocyte marker (CC1) (white arrows, tdT$^+$/PDGFRα$^+$ cells; blue arrows, tdT$^+$/CC1$^+$ cells). (*H*) Quantification of the percentage of tdT$^+$/PDGFRα$^+$ (OPCs), tdT$^+$/CC1$^+$ (oligodendrocytes), or tdT$^+$/PDGFRα$^+$/CC1$^+$ cells in the OB of WT and CKO mice at 90 dpi, suggesting mutant OPCs cannot differentiate effectively (n = 4 CKO and 3 WT mice). (*I*) Location of images shown in *F* and *G* and diagram of experimental procedure. Error bars represent SEM and statistical significance was determined by Student t test (*P < 0.05; **P < 0.01; ***P < 0.001). (Scale bars, 50 μm.)

not oligodendrogliomas based on the presence of angular, pleomorphic, rather than rounded, isomorphic nuclei and the lack of perinuclear halos or branched capillaries (Fig. 3*D*) (39, 40). The engraftment of tumor cells into the brains of NOD/SCID mice consistently gave rise to large, invasive secondary and tertiary tumors after 35–50 d (Table S1), confirming the malignancy of OPC-derived gliomas. Additionally, tumor cells cultured in clonal conditions exhibited self-renewing and multilineage differentiation potential (Fig. S3 *A–D*), suggesting the existence of tumor-propagating cells within adult OPC-derived gliomas. Therefore, we conclude that even relatively quiescent OPCs in a fully mature brain can give rise to glioma.

Interestingly, we noticed that tumors were not randomly distributed, despite equal distribution of mutant OPCs in all brain regions (Fig. 1*B*). Because it is difficult to pinpoint the anatomical origin of late-stage tumors due to their large size and infiltrative nature, we collected a set of brains at 120 dpi, when tumors are small, to quantify tumor frequency at distinct locations. The most common location was the OB (40%), followed by the habenula, a small region in the dorsal thalamus (25%), piriform cortex/amygdala (15%), and the space between the hypothalamus and the base of the skull (15%) (Fig. 3 *B* and *C* and Table S1). Altogether, we conclude that OPCs in the adult brain can exit their quiescent state and give rise to malignant anaplastic gliomas upon *p53/NF1* deletion.

Adult-Induced Gliomas Are Similar to Human Proneural Glioma and Maintain OPC Features. Recent studies have used genomic and transcriptomic approaches to define glioma subtypes within

pathologically indistinguishable tumor samples (41–46). These molecular classifications provide valuable insight for prognostic predictions and development of targeted therapies and emphasize the importance of matching distinct mouse glioma models to human subtypes. Therefore, we used microarray data to compare the transcriptional profile of 12 adult OPC-derived gliomas to that of human GBM samples by single sample Gene Set Enrichment Analysis (ssGSEA), which uses predefined sets of genes to determine the relative similarity between samples (Fig. 3*E*). The gliomas selected for analysis were large, terminal tumors that sometimes spanned several brain regions but likely originated in the OB (tumors 1, 3, 7, and 8), thalamus (tumor 10), piriform cortex/amygdala (tumors 2, 4, 5, and 9), and base of the skull (tumor 6), as well as two secondary tumors grafted from the OB and cortex/amygdala into the striatum (tumors 11 and 12, respectively; Table S1). We found that, regardless of anatomical origin or age of induction, most tumors from our model resemble the proneural subtype of human GBM (46), although some could not be unambiguously identified as proneural or classical (tumors 5–8; Fig. 3*E*). Consistent with their proneural signature, our adult-induced gliomas were similar to OPCs, but not neurons or astrocytes (Fig. 3*E* and Fig. S3 *E–I*) (46). Markers of pericytes and hemangiopericytomas (47) were also absent from these gliomas, consistent with their OPC origin (Fig. S3*I*). Interestingly, although many GFAP$^+$ cells were detected within the tumor masses, these were not tdT$^+$ (Fig. S3*H*), indicating that they are most likely local reactive astrocytes. These data concur with our previous findings with neonatal OPC-derived tumors (14) (Fig. 3*E*), suggesting that gliomas originated from *p53*/*NF1*-null OPCs generally belong to the proneural subtype regardless of the timing of mutations.

Adult OPC Gliomagenesis Follows a Multistep Process of Reactivation, Dormancy, and Malignancy. Having confirmed the transformation capability of adult OPCs, we next investigated how these rarely dividing progenitors become reactivated. To pinpoint the timing of OPC reactivation, we quantified both proliferative rate and total number of OPCs at several time points during the premalignant phase (preceding a detectable tumor). We initially focused on the OB, where gliomas most commonly develop in our model (Fig. 4 *A–E*). Before Tmx is given (0 dpi), WT and CKO OPCs have equally low proliferative rates. Just 12 d after Tmx (12 dpi), the proliferative rate of mutant OPCs increased to perinatal levels (54.9 ± 3.6% SEM; $n = 3$), but then quickly decreased to below WT levels at 50 dpi and remained low even at 90 dpi, just 30 d before gliomas begin to appear (Fig. 4*C*). As a consequence of reactivation, the number of tdT$^+$ mutant OPCs rose sharply in the first 12 d after Tmx administration. Surprisingly, the number of mutant OPCs continued to expand long after cells returned to WT proliferation levels (Fig. 4*D*), likely due to defects in differentiation of mutant OPCs (see below). In contrast, the number of labeled WT OPCs remained constant (Fig. 4*D*). Interestingly, we observed similar proliferation and cell number dynamics not only in other tumor hot spots (habenula), but also in regions where gliomas did not normally form (cingulate/motor cortex and corpus callosum; Fig. S4 *A–F*) except proliferation in the corpus callosum, which was identical in WT and CKO mice. Overall, these results suggest that additional events are needed for malignant transformation.

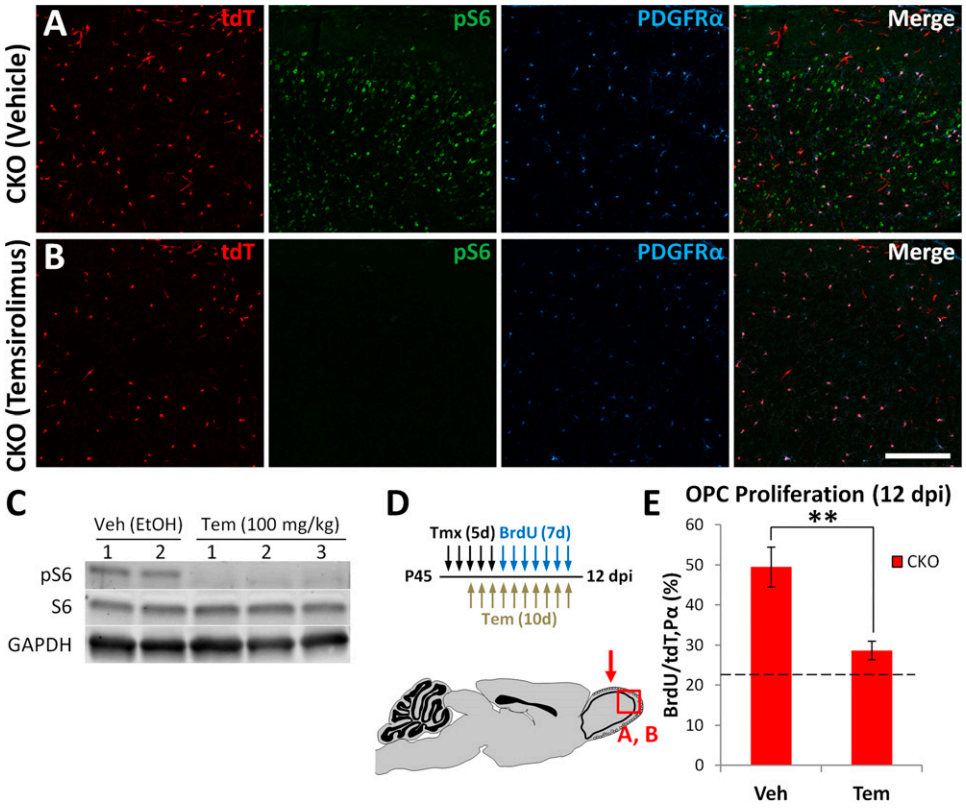

Fig. 5. mTOR signaling is necessary for mutant OPC reactivation. (*A* and *B*) Immunostaining of the OB of CKO mice treated with vehicle or temsirolimus, showing that the levels of phospho-S6 (pS6, mTOR downstream target) are drastically reduced by the drug. (*C*) Western blot for pS6 and total S6 protein in the OB, showing temsirolimus blocks phosphorylation of S6 by mTOR. Mice were treated for 10 (*A* and *B*) or 5 (*C*) d and then killed 4 h after the last dose. (*D*) Diagrams of experimental procedure and brain region analyzed (red arrow). (*E*) Quantification of the fraction of proliferating tdT$^+$ OPCs at 12 dpi in the OB of CKO mice treated with vehicle (Veh, control) or temsirolimus (Tem). Tem significantly decreases mutant OPC proliferation to WT adult OPC proliferation levels (dotted line) (Veh, $n = 3$; Tem, $n = 4$; $^{**}P < 0.01$). (Scale bar, 100 μm.)

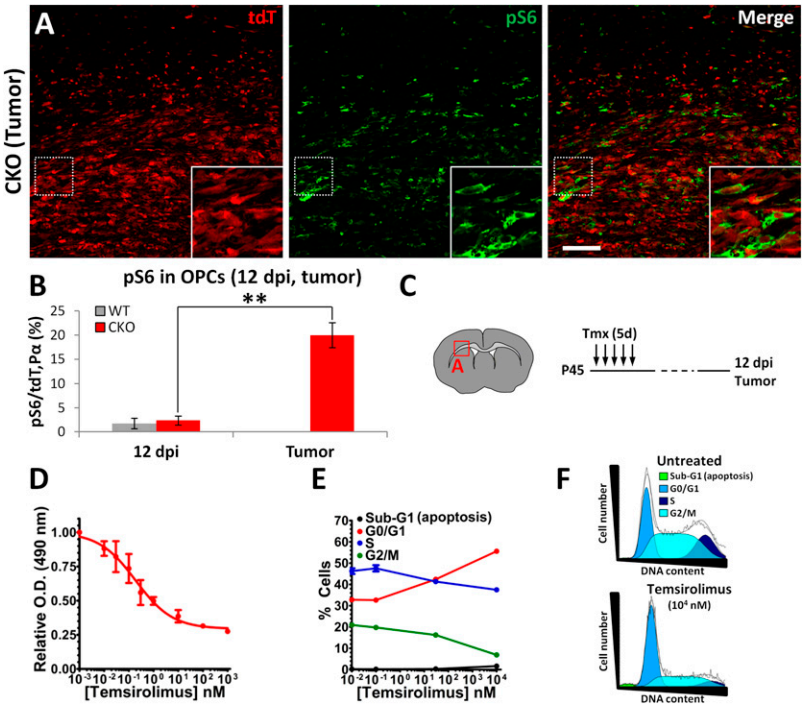

Fig. 6. mTOR signaling rises dramatically in malignant OPCs and is critical for glioma cell proliferation. (*A*) Immunostaining for phospho-S6 (pS6, mTOR target) in glioma tissue. (*B*) Quantification of the percentage of OPCs (tdT^+/$PDGFR\alpha^+$) and OPC-derived glioma cells (tdT^+ cells in tumor mass, typically all $PDGFR\alpha^+$ as seen on Fig. S6*D*; adjacent section of tumor in *A* and Fig. S3*F*) labeled with pS6, indicating higher levels of mTOR signaling in glioma cells ($n = 3$; $^{**}P < 0.01$). (*C*) Diagrams of location of image shown in *A* and experimental procedure. (*D*) Cellular viability assay of cultured glioma cells treated with temsirolimus, revealing a significant impact of this mTOR inhibitor on glioma cell growth in vitro. (*E*) Quantification of the fraction of glioma cells at different phases of the cell cycle (G0/G1, S, G2/M) and apoptosis (sub-G1) after exposure to increasing doses of temsirolimus, showing an increase in G0/G1 and decrease in G2/M that suggests G1 arrest. (*F*) DNA content distribution of untreated and temsirolimus-treated tumor cells, illustrating the drug-induced cell cycle arrest at G1 (jagged black line, actual data curve; smooth black line, fitted data curve; colored areas, cells presumed to be in different cell cycle stages, as per color code). (Scale bar, 100 μm.)

In addition to proliferation, the differentiation of OPCs into mature oligodendrocytes also affects their homeostatic balance. To determine whether *p53/NF1* mutations perturb OPC differentiation, we quantified the percentage of tdT^+ cells expressing PDGFRα (OPCs) or CC1 (oligodendrocytes) in the OB of WT and CKO mice at 90 dpi (Fig. 4 *F–I*). Compared with WT mice, CKO mice had significantly more tdT^+/$PDGFR\alpha^+$ cells and significantly fewer tdT^+/$CC1^+$ cells, indicating an impairment in OPC differentiation. As with proliferation, impaired differentiation was observed in all regions tested (Fig. S4*G*), including the corpus callosum, which could explain the increase in OPC numbers despite a lack of hyperproliferation in that region. Therefore, compromised differentiation of mutant OPCs, together with the early spike in proliferation, likely contributes to their continuous expansion throughout the premalignant phase, eventually leading to glioma. Importantly, OPCs mutated at P180 exhibited the same hyperproliferative (49% vs. 20% $BrdU^+$, $P < 0.01$) and undifferentiated (88% vs. 72% $PDGFR\alpha^+$, $P < 0.01$) behaviors at 12 dpi ($n = 3$), indicating that OPC reactivation competence is not lost over time. In summary, we found that gliomagenesis from adult OPCs involves multiple steps of cellular behavior alternations, including robust but transient reactivation in all brain regions immediately after mutagenesis, followed by slow but steady mutant cell expansion during a long period of apparent dormancy, and ending with sudden malignant transformation.

mTOR Inhibition Blocks Mutant OPC Reactivation Step. To study the molecular nature of the reactivation step, we focused on the mTOR signaling pathway, which has recently emerged as a key mechanism in the reactivation of quiescent neural, hematopoietic, and muscle stem cells (48–51) and is known to play a role in OPC proliferation and differentiation (27–30, 52). Therefore, we decided to test its involvement in mutation-induced OPC reactivation by administering the mTOR inhibitor temsirolimus throughout the 12 dpi period. The effectiveness of target inhibition in the brain was confirmed by immunostaining and Western blot (Fig. 5 *A–C*), both of which showed that brains of mice treated with temsirolimus have drastically reduced levels of phosphorylated S6 ribosomal protein (pS6), a downstream target of mTOR. Quantification of proliferation showed that OPCs in CKO mice treated with temsirolimus no longer underwent the characteristic 12 dpi spike, but instead remained at WT levels (Fig. 5*E*). Total OPC numbers were also reduced by mTOR inhibition (Fig. S5). These results suggest that mTOR signaling is necessary for the early reactivation of mutant OPCs.

mTOR Signaling Rises Dramatically in Malignant OPCs and Is Critical for Glioma Cell Proliferation. As our data above implicate mTOR signaling in the initial reactivation step of the premalignant phase, we next investigated whether this pathway is necessary at the malignant phase as well. We first quantified the percentage of $pS6^+$ OPCs at premalignant and malignant stages. We found that most $pS6^+$ cells in the adult OB are neurons (Fig. S6*A*), and that, unexpectedly, only 2% of OPCs are $pS6^+$ in WT or CKO mice at 12 dpi (Fig. 6*B* and Fig. S6 *B* and *C*), perhaps due to low levels of mTOR signaling (*Discussion*). In stark contrast, the percentage of $pS6^+$ OPCs increased drastically to 20% in the tumor mass (Fig. 6 *A* and *B*). We observed the same trend when staining for the phosphorylated form of another mTOR downstream target, 4E-binding protein 1 (4E-BP1), which was rarely seen before malignancy but quite common in tumor cells (Fig. S6*D*). Therefore, mTOR signaling appears to be highly up-regulated in malignant OPCs.

To test the role of mTOR signaling in OPC-derived glioma cells, we cultured cells from one of our primary gliomas with temsirolimus. Tumor cell growth was acutely sensitive to this mTOR inhibitor at doses that inhibited S6 and 4E-BP1 phosphorylation (Fig. 6*D* and Fig. S6*F*). Cell cycle analysis by flow cytometry demonstrated that this effect was due to cell cycle arrest at the G1 stage (Fig. 6 *E* and *F*), consistent with the known roles of mTOR signaling in promoting cell cycle progression at the G1 to S transition (53). These results were confirmed with EdU (5-ethynyl-2′-deoxyuridine) quantifications by immunostaining, as well as using another mTOR inhibitor (rapamycin, from which temsirolimus is derived) and another primary glioma cell line (Fig. S6 *G–I*). We conclude that OPC-derived glioma cells greatly increase cell intrinsic mTOR signaling, which is important for their proliferation.

Discussion

A deep understanding of the timing and process of gliomagenesis should greatly facilitate the development of effective therapies and biomarkers for early detection. We developed a genetic mouse model with both cell type specificity and temporal control to study gliomagenesis from adult OPCs for the first time. Using this model, we showed that quiescent adult OPCs can be reactivated upon mutagenesis and transform into malignant gliomas that preferentially develop in defined locations. Time course analysis revealed a surprising, multistep behavior of mutant OPC reactivation, dormancy, and malignant transformation. Finally, we uncovered an important role for mTOR signaling at both early and late stages of gliomagenesis.

Although previous studies have suggested NSCs as the cell of origin for glioma (35, 54, 55), our prior work showed that even though introducing mutations in NSCs can lead to glioma, malignant transformation only occurs in OPCs, thus warranting a distinction between cell of mutation (NSCs) and cell of origin (OPCs) (14). It remains possible that additional cell types also act as a cell of origin, such as the OPC-like type C* cells described by others (56), or that different glioma subtypes are derived from different cells of origin, such as low-grade ocular tract gliomas, which might not be OPC-derived (57). Nonetheless, overwhelming evidence now supports OPCs as a cell of origin for glioma (14, 58–64). However, these studies either introduced oncogenes into OPCs early in development, as in our previous work (14), or did not use lineage tracing tools (58, 59). Thus, it is possible that the gliomagenic potential of OPCs could be dependent on their active perinatal state (65, 66) and that adult OPCs may not be transformable because they rarely divide (9, 17–21). Our current study convincingly resolved this issue by introducing mutations specifically into adult OPCs and demonstrating their capacity for transformation. Because most human malignant gliomas occur in elderly adults (25), our findings not only firmly establish OPCs as a cell of origin for glioma but also highlight the clinical relevance of this discovery.

Because gliomas have no known morphologically detectable preneoplastic lesions, it is difficult to study early events before final malignancy. Taking advantage of the lineage marker tdTomato in our mouse model, we followed the progression of gliomagenesis and found that it is not a linear process but rather marked by successive steps of reactivation, dormancy, and malignant transformation. The reactivation step is likely caused by signaling perturbations due to the acute loss of *p53* and *NF1*, but mutant OPCs quickly return to quiescence/dormancy. This dormancy could be due to cell intrinsic tumor suppressor mechanisms activated by *NF1* loss of function (67) or cell extrinsic mechanisms including competition for limited trophic support or cell contact-mediated growth inhibition as the number of mutant OPCs increases (68). Interestingly, mutant OPCs continue to accumulate throughout this dormant period, likely due to an inability to differentiate into oligodendrocytes. This lack of differentiation distinguishes mutation-induced from physiological or injury-induced OPC reactivation, which is a controlled process ending with differentiation of the reactivated cells (22–24). Eventually, one or more mutant cells exit dormancy to undergo malignant transformation, triggering the formation of a tumor mass. The mechanism for malignant transformation remains unclear, but likely depends on additional mutations that allow OPCs to overcome the barriers that kept them dormant after the initial reactivation. Overall, the discovery of a stepwise process of gliomagenesis provides multiple new potential therapeutic approaches, such as early interventions to prevent OPC reactivation or to induce their differentiation, which might help prevent gliomagenesis by halting the progression toward malignant transformation.

The malignant transformation step could also be dependent on niche properties of certain brain regions, as suggested by our finding that malignant gliomas develop preferentially in specific locations. In fact, regional differences in the expression of signaling molecules have been suggested to account for the unique properties of CNS progenitors in those areas as well as their response to oncogenic mutations (12, 13, 69, 70). Alternatively, OPCs themselves could have heterogeneous characteristics depending on the brain region (52, 71, 72), which could influence their transformation potential. Future studies investigating these possibilities might provide critical insights into what drives gliomagenesis.

The mTOR pathway has recently emerged as a key mechanism in stem cell reactivation. In *Drosophila*, nutrient-stimulated TOR signaling reactivates quiescent neural stem cells during the embryo-to-larva transition (51). In mammals, adult hematopoietic stem cells are kept quiescent via TSC1-mediated inhibition of mTOR (48, 49), and quiescent adult muscle stem cells display an mTOR-dependent increase in proliferation and cell size after injury (50). In OPCs, mTOR signaling promotes proliferation and differentiation during development (27–30, 52), and its activity is blocked by p53 via stress-induced up-regulation of mTOR inhibitors (73) and NF1 via Ras inhibition (74, 75). Therefore, mTOR could be part of the molecular mechanism behind mutation-induced adult OPC reactivation. Consistent with its role in development, we found that pharmacological inhibition of mTOR signaling with temsirolimus decreased WT adult OPC proliferation (22.6% vs. 5.8% $BrdU^+$, $P = 0.004$) and differentiation (55.6% vs. 65.6% $PDGFR\alpha^+$, $P = 0.01$). Importantly, temsirolimus treatment also blocked mutant OPC hyperproliferation at 12 dpi, indicating that this pathway is necessary for the initial reactivation step. Interestingly, temsirolimus did not affect mutant OPC differentiation, likely because this process was already impaired by the loss of *p53* and *NF1*. Because the mTOR pathway is also active in a variety of cancers (76), we investigated its role in malignant OPC proliferation and found that blocking mTOR strongly inhibits tumor cell growth. Overall, our results show that mTOR signaling is involved in both the initial reactivation of *p53*/*NF1*-mutant OPCs as well as the uncontrolled proliferation of OPC-derived gliomas. These findings should provide the rationale and facilitate the regimen design for an effective use of the next generation of mTOR inhibitors currently being developed (76). Specifically, treatment early in the course of disease could be beneficial and could prevent low- to high-grade glioma progression. Due to the complex mutational landscape of malignant gliomas (15, 16), such treatments would likely be most effective as part of a combinatorial strategy in which multiple deregulated pathways would be targeted.

Given the clear effect of the mTOR inhibitor temsirolimus in blocking OPC proliferation at 12 dpi, we were surprised to find that very few OPCs at this time point have detectable levels of pS6 or p4E-BP1, both downstream targets of mTOR and common indicators of pathway activity. This lack of pS6 or p4E-BP1 signals could be due to mTOR signaling occurring below detection levels in these cells, which could be necessary to avoid cellular senescence and/or apoptosis, as reported for Kras and Myc oncogene signaling (77–81). Alternatively, mTOR signaling in premalignant OPCs could occur through untested downstream targets or temsirolimus could exert its antiproliferative effect via mTOR-independent mechanisms (82, 83). One intriguing possibility is that mTOR signaling in $pS6^+$ cells in the brain could have a paracrine effect on OPCs, as occurs in nutrient-dependent reactivation of quiescent *Drosophila* neural stem cells (51). Nevertheless, once mutant OPCs become malignant, mTOR's proliferative role is likely cell autonomous based on their robust labeling with pS6 and p4E-BP1 in vivo and their sensitivity to temsirolimus in vitro. Although its exact mode of action warrants further investigation, temsirolimus prevents both mutant OPC reactivation and tumor cell proliferation, pinpointing mTOR signaling as an integral part of the gliomagenic process.

In summary, our results have solidified the role of OPCs as a cell of origin for glioma and shed light on the poorly understood premalignant phase of gliomagenesis. Our findings have also led

to important questions. How do mutant OPCs become dormant after the initial reactivation? What causes their eventual escape from the dormant state to form a tumor? What mechanisms are responsible for tumor hot spots? The answers to these questions will continue to advance our understanding of glioma and will hopefully bring us closer to effective treatments.

Materials and Methods

Additional details are available in *SI Materials and Methods*.

In Vivo Drug Delivery. All mice were given daily tamoxifen doses of 200 mg/kg for several consecutive days (2 d for perinatal mice, 5 d for adult mice, except mice used for dosage curve, Fig. S1*A*; and mice used for detection of new OB neurons, Fig. S2). BrdU was given by i.p. (adult mice) or s.c. (perinatal mice) injection at 50 mg/kg. Mice were given one injection per day for 7 d and killed 24 h after the last injection. Temsirolimus (CCI-779; Selleckchem) was injected i.p. at 100 mg/kg (40 μL/g body weight) daily for 10 d. Mice were killed 4 h after the last dose was delivered.

Tumor Cell Grafting. CKO mice suspected of having a primary brain tumor were decapitated to dissect the tumor mass, which was then dissociated to a single cell suspension; 10^5 cells were immediately grafted into the striatum of each NOD-SCID mouse.

Sphere-Forming Assay. Cultured tumor cells were plated onto nonadhering 96-well plates and 60-mm dishes at clonal density (100 cells/μL, 10^4 cells/well for 96-well plates, 5×10^5 cells/dish for 60-mm dishes) in medium supplemented with EGF (20 ng/mL) and FGF2 (10 ng/mL). To differentiate, spheres were placed on matrigel-coated plates in medium without EGF/FGF2 and with 1% FBS for 6 d.

Microarray Analysis and Single Sample Gene Set Enrichment Analysis. 44K Mouse Development Oligo Microarrays from Agilent Technologies were used to analyze total RNA extracted from bulk tumor tissue that was hybridized against a common reference sample of RNA pooled from four WT P17 mouse brain neocortices. Single sample GSEA was performed as described elsewhere (46). To compare tumor samples to the different mouse brain cell types, data from a previous publication (84) was downloaded and preprocessed as described previously (46) into sets of 250 variably expressed gene clusters. The clusters used in the present study contained postnatal day 16 myelin oligodendrocytes ($n = 4$), postnatal day 6–7 OPCs ($n = 2$), postnatal day 7 neurons ($n = 4$), and postnatal day 17–30 astrocytes ($n = 6$). Gene sets for four previously described GBM subtypes (46) were defined by selecting the top 250 marker genes as provided.

Cell Growth Assay. OPC-derived glioma cells were treated with increasing concentrations of temsirolimus (Selleckchem), rapamycin (Sigma-Aldrich), or DMSO (untreated). Growth of treated vs. untreated cells was determined at 5 d after treatment using CellTiter 96 Aqueous One Solution Cell Proliferation Assay (MTS; Promega). Cell growth was determined in quadruplicate per drug concentration and data pooled from two independent experiments.

Cell Cycle Analysis. OPC-derived glioma cells were treated with increasing concentrations of temsirolimus, harvested 48 h later, and stained with the Guava Cell Cycle Reagent (EMD Millipore), and DNA content was determined using a Guava EasyCyte Plus flow cytometer. Data were obtained in triplicate per drug concentration and data pooled from two independent experiments. For quantification of proliferation by EdU incorporation, tumor cells were cultured for 3 d in 100 nM temsirolimus and then given EdU for 8 h and immediately fixed in 4% (wt/vol) formaldehyde.

Immunoblots. For in vivo experiments, OB tissue from WT mice treated for 5 d with vehicle or temsirolimus was collected 4 h after the last dose and immediately flash-frozen in liquid nitrogen until further processing. For in vitro experiments, OPC-derived glioma cells treated with temsirolimus for 24 h were harvested and lysed. For both types of experiments, protein concentration was quantified using the BCA assay (BioRad), and immunoblots were performed by resolving equal amounts of protein by gradient [8–16% (vol/vol)] SDS/PAGE (Bio-Rad) and transferred to PVDF membranes (EMD Millipore) for immunodetection.

Quantifications and Statistics. Cryosections (16 μm thick; or 30-μm-thick vibratome sections for type A and C cell quantifications) were imaged with a confocal microscope. The significance of the quantification data was calculated by Student *t* test. All error bars represent SEM.

ACKNOWLEDGMENTS. We thank A. Henner for technical support and C. Liu, P. Gonzalez, M. Yao, M. Kohwi, D. Brautigan, Y. Zhu, K. Park, J. Kim, and S. Gutkind for critical comments on the manuscript. This work was supported in part by National Institutes of Health Grant R01-CA136495 (to H.Z.), Medical Research Program of W. M. Keck Foundation (H.Z.), and the University of North Carolina Cancer Research Fund (C.R.M.). J.E.H. was supported by the University of Oregon Summer Program in Undergraduate Research. C.R.M. is a Damon Runyon-Genentech Clinical Investigator supported in part by a Clinical Investigator award from the Damon Runyon Cancer Research Foundation (CI-45-09). R.S.M. is a Robert H. Wagner Scholar in the UNC Molecular and Cellular Pathology Graduate Program and a trainee in the UNC Graduate Training Program in Translational Medicine, supported in part by the Howard Hughes Medical Institute. H.Z. is a Pew Scholar in Biomedical Sciences, supported by the Pew Charitable Trusts.

1. Cheung TH, Rando TA (2013) Molecular regulation of stem cell quiescence. *Nat Rev Mol Cell Biol* 14(6):329–340.
2. Matsumoto A, Nakayama KI (2013) Role of key regulators of the cell cycle in maintenance of hematopoietic stem cells. *Biochim Biophys Acta* 1830(2): 2335–2344.
3. Montarras D, L'honoré A, Buckingham M (2013) Lying low but ready for action: The quiescent muscle satellite cell. *FEBS J* 280(17):4036–4050.
4. Udagawa T (2008) Tumor dormancy of primary and secondary cancers. *APMIS* 116(7-8):615–628.
5. Valcourt JR, et al. (2012) Staying alive: Metabolic adaptations to quiescence. *Cell Cycle* 11(9):1680–1696.
6. Maslov AY, Barone TA, Plunkett RJ, Pruitt SC (2004) Neural stem cell detection, characterization, and age-related changes in the subventricular zone of mice. *J Neurosci* 24(7):1726–1733.
7. Molofsky AV, et al. (2006) Increasing p16INK4a expression decreases forebrain progenitors and neurogenesis during ageing. *Nature* 443(7110):448–452.
8. Pietras EM, Warr MR, Passegué E (2011) Cell cycle regulation in hematopoietic stem cells. *J Cell Biol* 195(5):709–720.
9. Psachoulia K, Jamen F, Young KM, Richardson WD (2009) Cell cycle dynamics of NG2 cells in the postnatal and ageing brain. *Neuron Glia Biol* 5(3-4):57–67.
10. Chen W, et al. (2008) Malignant transformation initiated by Mll-AF9: Gene dosage and critical target cells. *Cancer Cell* 13(5):432–440.
11. Johnson RA, et al. (2010) Cross-species genomics matches driver mutations and cell compartments to model ependymoma. *Nature* 466(7306):632–636.
12. Lee Y, Gianino SM, Gutmann DH (2012) Innate neural stem cell heterogeneity determines the patterning of glioma formation in children. *Cancer Cell* 22(1): 131–138.
13. Lee Y, Yeh TH, Emnett RJ, White CR, Gutmann DH (2010) Neurofibromatosis-1 regulates neuroglial progenitor proliferation and glial differentiation in a brain region-specific manner. *Genes Dev* 24(20):2317–2329.
14. Liu C, et al. (2011) Mosaic analysis with double markers reveals tumor cell of origin in glioma. *Cell* 146(2):209–221.
15. Cancer Genome Atlas Research Network (2008) Comprehensive genomic characterization defines human glioblastoma genes and core pathways. *Nature* 455(7216): 1061–1068.
16. Parsons DW, et al. (2008) An integrated genomic analysis of human glioblastoma multiforme. *Science* 321(5897):1807–1812.
17. Shi J, Marinovich A, Barres BA (1998) Purification and characterization of adult oligodendrocyte precursor cells from the rat optic nerve. *J Neurosci* 18(12):4627–4636.
18. Wolswijk G, Noble M (1989) Identification of an adult-specific glial progenitor cell. *Development* 105(2):387–400.
19. Young KM, et al. (2013) Oligodendrocyte dynamics in the healthy adult CNS: Evidence for myelin remodeling. *Neuron* 77(5):873–885.
20. Belachew S, et al. (2002) Cyclin-dependent kinase-2 controls oligodendrocyte progenitor cell cycle progression and is downregulated in adult oligodendrocyte progenitors. *J Neurosci* 22(19):8553–8562.
21. Lin G, Mela A, Guilfoyle EM, Goldman JE (2009) Neonatal and adult O4(+) oligodendrocyte lineage cells display different growth factor responses and different gene expression patterns. *J Neurosci Res* 87(15):3390–3402.
22. Gibson EM, et al. (2014) Neuronal activity promotes oligodendrogenesis and adaptive myelination in the mammalian brain. *Science* 344(6183):1252304.
23. Franklin RJ, Ffrench-Constant C (2008) Remyelination in the CNS: From biology to therapy. *Nat Rev Neurosci* 9(11):839–855.
24. McTigue DM, Tripathi RB (2008) The life, death, and replacement of oligodendrocytes in the adult CNS. *J Neurochem* 107(1):1–19.
25. Dolecek TA, Propp JM, Stroup NE, Kruchko C (2012) CBTRUS statistical report: Primary brain and central nervous system tumors diagnosed in the United States in 2005-2009. *Neuro-oncol* 14(Suppl 5):v1–v49.
26. Li L, Bhatia R (2011) Stem cell quiescence. *Clin Cancer Res* 17(15):4936–4941.
27. Baron W, Metz B, Bansal R, Hoekstra D, de Vries H (2000) PDGF and FGF-2 signaling in oligodendrocyte progenitor cells: Regulation of proliferation and differentiation by multiple intracellular signaling pathways. *Mol Cell Neurosci* 15(3):314–329.

28. Guardiola-Diaz HM, Ishii A, Bansal R (2012) Erk1/2 MAPK and mTOR signaling sequentially regulates progression through distinct stages of oligodendrocyte differentiation. *Glia* 60(3):476–486.
29. Tyler WA, et al. (2009) Activation of the mammalian target of rapamycin (mTOR) is essential for oligodendrocyte differentiation. *J Neurosci* 29(19):6367–6378.
30. Zou J, et al. (2011) Rheb1 is required for mTORC1 and myelination in postnatal brain development. *Dev Cell* 20(1):97–108.
31. Paugh BS, et al. (2010) Integrated molecular genetic profiling of pediatric high-grade gliomas reveals key differences with the adult disease. *J Clin Oncol* 28(18):3061–3068.
32. Sturm D, et al. (2014) Paediatric and adult glioblastoma: Multiform (epi)genomic culprits emerge. *Nat Rev Cancer* 14(2):92–107.
33. Zhu X, et al. (2011) Age-dependent fate and lineage restriction of single NG2 cells. *Development* 138(4):745–753.
34. Dawson MR, Polito A, Levine JM, Reynolds R (2003) NG2-expressing glial progenitor cells: an abundant and widespread population of cycling cells in the adult rat CNS. *Mol Cell Neurosci* 24(2):476–488.
35. Alcantara Llaguno S, et al. (2009) Malignant astrocytomas originate from neural stem/progenitor cells in a somatic tumor suppressor mouse model. *Cancer Cell* 15(1):45–56.
36. Ihrie RA, Alvarez-Buylla A (2011) Lake-front property: A unique germinal niche by the lateral ventricles of the adult brain. *Neuron* 70(4):674–686.
37. Petreanu L, Alvarez-Buylla A (2002) Maturation and death of adult-born olfactory bulb granule neurons: Role of olfaction. *J Neurosci* 22(14):6106–6113.
38. Winner B, Cooper-Kuhn CM, Aigner R, Winkler J, Kuhn HG (2002) Long-term survival and cell death of newly generated neurons in the adult rat olfactory bulb. *Eur J Neurosci* 16(9):1681–1689.
39. Louis DN, Ohgaki H, Wiestler OD, Cavenee WK (2007) *WHO Classification of Tumours of the Central Nervous System* (International Agency for Research on Cancer, World Health Organization, Geneva), 4th Ed, p 309.
40. Sarkar C, Jain A, Suri V (2009) Current concepts in the pathology and genetics of gliomas. *Indian J Cancer* 46(2):108–119.
41. Brennan C, et al. (2009) Glioblastoma subclasses can be defined by activity among signal transduction pathways and associated genomic alterations. *PLoS ONE* 4(11):e7752.
42. Cooper LA, et al. (2010) The proneural molecular signature is enriched in oligodendrogliomas and predicts improved survival among diffuse gliomas. *PLoS ONE* 5(9):e12548.
43. Freije WA, et al. (2004) Gene expression profiling of gliomas strongly predicts survival. *Cancer Res* 64(18):6503–6510.
44. Nutt CL, et al. (2003) Gene expression-based classification of malignant gliomas correlates better with survival than histological classification. *Cancer Res* 63(7):1602–1607.
45. Phillips HS, et al. (2006) Molecular subclasses of high-grade glioma predict prognosis, delineate a pattern of disease progression, and resemble stages in neurogenesis. *Cancer Cell* 9(3):157–173.
46. Verhaak RG, et al.; Cancer Genome Atlas Research Network (2010) Integrated genomic analysis identifies clinically relevant subtypes of glioblastoma characterized by abnormalities in PDGFRA, IDH1, EGFR, and NF1. *Cancer Cell* 17(1):98–110.
47. Armulik A, Genové G, Betsholtz C (2011) Pericytes: Developmental, physiological, and pathological perspectives, problems, and promises. *Dev Cell* 21(2):193–215.
48. Chen C, et al. (2008) TSC-mTOR maintains quiescence and function of hematopoietic stem cells by repressing mitochondrial biogenesis and reactive oxygen species. *J Exp Med* 205(10):2397–2408.
49. Gan B, et al. (2008) mTORC1-dependent and -independent regulation of stem cell renewal, differentiation, and mobilization. *Proc Natl Acad Sci USA* 105(49):19384–19389.
50. Rodgers JT, et al. (2014) mTORC1 controls the adaptive transition of quiescent stem cells from G0 to G(Alert). *Nature* 510(7505):393–396.
51. Sousa-Nunes R, Yee LL, Gould AP (2011) Fat cells reactivate quiescent neuroblasts via TOR and glial insulin relays in Drosophila. *Nature* 471(7339):508–512.
52. Hill RA, Patel KD, Medved J, Reiss AM, Nishiyama A (2013) NG2 cells in white matter but not gray matter proliferate in response to PDGF. *J Neurosci* 33(36):14558–14566.
53. Fingar DC, et al. (2004) mTOR controls cell cycle progression through its cell growth effectors S6K1 and 4E-BP1/eukaryotic translation initiation factor 4E. *Mol Cell Biol* 24(1):200–216.
54. Zheng H, et al. (2008) p53 and Pten control neural and glioma stem/progenitor cell renewal and differentiation. *Nature* 455(7216):1129–1133.
55. Zhu Y, et al. (2005) Early inactivation of p53 tumor suppressor gene cooperating with NF1 loss induces malignant astrocytoma. *Cancer Cell* 8(2):119–130.
56. Wang Y, et al. (2009) Expression of mutant p53 proteins implicates a lineage relationship between neural stem cells and malignant astrocytic glioma in a murine model. *Cancer Cell* 15(6):514–526.
57. Solga AC, Gianino SM, Gutmann DH (2014) NG2-cells are not the cell of origin for murine neurofibromatosis-1 (Nf1) optic glioma. *Oncogene* 33(3):289–299.
58. Assanah M, et al. (2006) Glial progenitors in adult white matter are driven to form malignant gliomas by platelet-derived growth factor-expressing retroviruses. *J Neurosci* 26(25):6781–6790.
59. Lei L, et al. (2011) Glioblastoma models reveal the connection between adult glial progenitors and the proneural phenotype. *PLoS ONE* 6(5):e20041.
60. Lindberg N, Kastemar M, Olofsson T, Smits A, Uhrbom L (2009) Oligodendrocyte progenitor cells can act as cell of origin for experimental glioma. *Oncogene* 28(23):2266–2275.
61. Masui K, et al. (2010) Glial progenitors in the brainstem give rise to malignant gliomas by platelet-derived growth factor stimulation. *Glia* 58(9):1050–1065.
62. Persson AI, et al. (2010) Non-stem cell origin for oligodendroglioma. *Cancer Cell* 18(6):669–682.
63. Sugiarto S, et al. (2011) Asymmetry-defective oligodendrocyte progenitors are glioma precursors. *Cancer Cell* 20(3):328–340.
64. Weiss WA, et al. (2003) Genetic determinants of malignancy in a mouse model for oligodendroglioma. *Cancer Res* 63(7):1589–1595.
65. Lei L, Canoll P (2011) MADM gives new insights into gliomagenesis. *J Mol Cell Biol* 3(5):273–275.
66. Sukhdeo K, Hambardzumyan D, Rich JN (2011) Glioma development: Where did it all go wrong? *Cell* 146(2):187–188.
67. Courtois-Cox S, et al. (2006) A negative feedback signaling network underlies oncogene-induced senescence. *Cancer Cell* 10(6):459–472.
68. Hughes EG, Kang SH, Fukaya M, Bergles DE (2013) Oligodendrocyte progenitors balance growth with self-repulsion to achieve homeostasis in the adult brain. *Nat Neurosci* 16(6):668–676.
69. Ihrie RA, et al. (2011) Persistent sonic hedgehog signaling in adult brain determines neural stem cell positional identity. *Neuron* 71(2):250–262.
70. Warrington NM, et al. (2010) Cyclic AMP suppression is sufficient to induce gliomagenesis in a mouse model of neurofibromatosis-1. *Cancer Res* 70(14):5717–5727.
71. Dimou L, Simon C, Kirchhoff F, Takebayashi H, Götz M (2008) Progeny of Olig2-expressing progenitors in the gray and white matter of the adult mouse cerebral cortex. *J Neurosci* 28(41):10434–10442.
72. Viganò F, Möbius W, Götz M, Dimou L (2013) Transplantation reveals regional differences in oligodendrocyte differentiation in the adult brain. *Nat Neurosci* 16(10):1370–1372.
73. Feng Z (2010) p53 regulation of the IGF-1/AKT/mTOR pathways and the endosomal compartment. *Cold Spring Harb Perspect Biol* 2(2):a001057.
74. Banerjee S, Crouse NR, Emnett RJ, Gianino SM, Gutmann DH (2011) Neurofibromatosis-1 regulates mTOR-mediated astrocyte growth and glioma formation in a TSC/Rheb-independent manner. *Proc Natl Acad Sci USA* 108(38):15996–16001.
75. Johannessen CM, et al. (2005) The NF1 tumor suppressor critically regulates TSC2 and mTOR. *Proc Natl Acad Sci USA* 102(24):8573–8578.
76. Zoncu R, Efeyan A, Sabatini DM (2011) mTOR: From growth signal integration to cancer, diabetes and ageing. *Nat Rev Mol Cell Biol* 12(1):21–35.
77. Feldser DM, et al. (2010) Stage-specific sensitivity to p53 restoration during lung cancer progression. *Nature* 468(7323):572–575.
78. Junttila MR, et al. (2010) Selective activation of p53-mediated tumour suppression in high-grade tumours. *Nature* 468(7323):567–571.
79. Murphy DJ, et al. (2008) Distinct thresholds govern Myc's biological output in vivo. *Cancer Cell* 14(6):447–457.
80. Rad R, et al. (2013) A genetic progression model of Braf(V600E)-induced intestinal tumorigenesis reveals targets for therapeutic intervention. *Cancer Cell* 24(1):15–29.
81. Sarkisian CJ, et al. (2007) Dose-dependent oncogene-induced senescence in vivo and its evasion during mammary tumorigenesis. *Nat Cell Biol* 9(5):493–505.
82. Galat A (2013) Functional diversity and pharmacological profiles of the FKBPs and their complexes with small natural ligands. *Cell Mol Life Sci* 70(18):3243–3275.
83. Romano MF, et al. (2004) Rapamycin inhibits doxorubicin-induced NF-kappaB/Rel nuclear activity and enhances the apoptosis of melanoma cells. *Eur J Cancer* 40(18):2829–2836.
84. Cahoy JD, et al. (2008) A transcriptome database for astrocytes, neurons, and oligodendrocytes: A new resource for understanding brain development and function. *J Neurosci* 28(1):264–278.
85. Doetsch F, García-Verdugo JM, Alvarez-Buylla A (1999) Regeneration of a germinal layer in the adult mammalian brain. *Proc Natl Acad Sci USA* 96(20):11619–11624.